AIAA-2001-1004

PREDICTION OF BUSINESS JET AIRLOADS USING THE OVERFLOW NAVIER-STOKES CODE

Elias Bounajem*
Cessna Aircraft Company, Wichita, Kansas 67215

and

Pieter G. Buning**
NASA Langley Research Center, Hampton, Virginia 23681

Abstract

The objective of this work is to evaluate the application of Navier-Stokes computational fluid dynamics technology, for the purpose of predicting off-design condition airloads on a business jet configuration in the transonic regime. The NASA Navier-Stokes flow solver OVERFLOW with Chimera overset grid capability, availability of several numerical schemes and convergence acceleration techniques was selected for this work. A set of scripts which have been compiled to reduce the time required for the grid generation process are described. Several turbulence models are evaluated in the presence of separated flow regions on the wing. Computed results are compared to available wind tunnel data for two Mach numbers and a range of angles-of-attack. Comparisons of wing surface pressure from numerical simulation and wind tunnel measurements show good agreement up to fairly high angles-of-attack.

Introduction

Computational Fluid Dynamics (CFD) technology has seen remarkable advances in the last few years. CFD is used today on a regular basis to support design efforts in such areas as aircraft design, propulsion system design and integration, combustion, ship design and the automotive industry, to name a few.

The aircraft industry is a primary customer of CFD technology. Depending on the task at hand, the aircraft designer has a wide range of sophistication to chose from. This range includes: full modeling of viscous effects as available in Navier-Stokes type codes; Euler codes, transonic small disturbances and full potential codes when viscous effects are not of primary influence; and finally, linearized potential flow codes for shock free flows or when only an approximate answer is being sought. These codes are implemented with different types of grids: multiblock, patched or overset grids if a structured grid approach is considered, Cartesian and unstructured grids for unstructured methods. The literature is rich with publications identifying the pros and cons of each of these methods.

The bulk of CFD work in the aircraft design arena has been in the cruise flight regime. Under these conditions, the airflow is still attached to the surface with small regions of separated flow, and CFD calculations are known to be quite reliable in predicting aircraft performance characteristics.

Areas which have not received as much attention are those that deviate from the

* Member, AIAA
**Associate Fellow, AIAA.

cruise condition. These situations are encountered when the entire flight envelope of the airplane is of interest. Here, combinations of angle-of-attack, Mach and Reynolds number can be challenging for any CFD code. High angle-of-attack will cause the flow to separate. As the high subsonic regime is approached, the flow will have numerous shock waves on the wing, pylon, etc. The interaction of shock waves with the boundary layer complicates flow patterns and makes CFD prediction significantly more difficult. With the presence of large separated flow regions, the focus shifts more and more towards turbulence modeling. Here, the validity of the model's underlying assumptions becomes critical to the quality of the solution the CFD code can provide.

The present work aims at evaluating the applicability of Navier-Stokes CFD technology to predict off-design airloads on a business jet configuration. OVERFLOW [1,10], a NASA research flow solver which uses the Chimera overset grid approach, has been selected for this evaluation. OVERFLOW offers a wide array of numerical schemes and turbulence models, and has been accepted throughout the aircraft industry as one of the leading Navier-Stokes codes available.

Grid Generation

The overset grid approach has the advantage of allowing grid generation of aircraft components separately, thus providing grids that conform to the component topology. Through a hole cutting procedure and boundary point interpolation, excess overlap between component grids is blanked out.

The geometry modeled here is a business jet configuration with aft fuselage mounted pylon/nacelles. Figure 1 shows the different surface grids that make up the current model. In all fifteen grids, including the outer box grids, were needed to define the geometry.

Surface Grids

The first step in the grid generation process is to generate surface grids for the various components. Five components were identified: wing, fuselage, pylon, nacelle and wing-body fairing. For the wing, pylon, and nacelle, the CATIA CAD model was imported in IGES format into the NASA Langley GridTool software [2], where a surface grid was generated. The fuselage surface grid was generated directly in CATIA to improve surface grid quality resulting from projection onto the original geometry. As for the wing-body fairing (Figure 2), it was deemed appropriate to represent it with a combination of collar grids and therefore no computational surface grid was generated for this component.

Collar Grids

The next step in the process is to make use of the collar grid approach [3] in the overlap region between the various components. This approach is used to ensure good quality grids in these areas, to allow for inter-grid communication through interpolation and to capture the viscous effects in the juncture all in the same grid. Collar grids are generated by identifying the intersection curve between components and growing a grid onto the adjacent components.

Collar grids were generated at the pylon-nacelle and pylon-fuselage junctures. For the wing-body fairing, a collar grid was generated at the fuselage-fairing intersection and at the wing-fairing intersection. A third grid originating at the model centerline covered the remainder of the fairing.

The NASA Ames Chimera Grid Tools (CGT) software package [4] was used to generate the collar grids, to add wakes to the wing and pylon grids, and to add a wing tip cap grid [14]. Another cap grid was required for the pylon shelf, which extended beyond the nacelle exhaust plane. To increase communication with the nacelle grid, the pylon cap grid was extended upstream and projected onto the nacelle surface (Figure 3).

Volume Grids

From the body-fitted surface grids, volume grids were generated with HYPGEN [5-6]. The initial spacing off the surface is equal to 0.00035 inches, which corresponds to a y^+

value of 1 at 10 percent chord from the wing leading edge.

Communication between the component grid outer boundaries, and extension of the computational domain to the far field is accomplished with two levels of Cartesian box grids, following an approach used for other geometries [7-8].

Grid Communication

The PEGSUS 4.0 code [9], developed by CALSPAN at AEDC, is used to remove excess overlap between grids and find interpolation stencils for inter-grid boundary points. This process effectively connects all of the overset component and box grids into one system.

Scripting the Process

It is recognized that this grid generation process is iterative. Several attempts may be made to ensure that the surface is adequately represented and that the number of orphan points, grid points with no adequate interpolation stencil, is minimized. Also, during development phase, the configuration is constantly changing as more refinements are introduced. With this in mind, a set of scripts that performs the tasks highlighted above is highly desirable. This allows for making changes to the various components and then regenerating the entire grid system with a minimum amount of user input.

The present work uses a modified set of scripts, originally developed for a generic business jet configuration. These scripts encompass surface grid generation and refinements, volume grid generation, hole cutting and interpolation stencil identification. An example illustrating the script approach is the generation of the wing-body fairing collar grids. As shown in Figure 4, this process starts with wing and fuselage surface grids, the fairing definition in the form of reference grids (created in GridTool from the IGES CAD definition), and grid lines representing the intersection of the fairing with each of the fuselage, wing, and symmetry plane.

The first step uses the SURGRD surface grid generation code [15] from CGT to create collar surface grids, shown in Figure 2. Second, volume grids are generated with HYPGEN. Finally, CGT utilities are used to add reflected symmetry planes and smooth the wake region of the wing-fairing collar.

Flow Solver

The OVERFLOW Navier-Stokes flow solver is used in this analysis. This code uses an implicit approximate factorization algorithm to solve the thin-layer formulation of the Navier-Stokes equations. For these calculations, central differencing with second- and fourth-order artificial dissipation is used for the Euler terms. Trial runs with Roe's upwind differencing scheme did not show improvement over central differencing. Local time stepping, grid sequencing, and multigrid are used to accelerate convergence [10].

While steady-state acceleration techniques were used for these simulations, the mid-range and high angle-of-attack cases were largely separated. Total lift coefficient varied by 0.02 from a mean value in some cases. It is recognized that a more thorough analysis of the unsteady aspect of these flowfields is needed; however, for the airloads analysis process only averaged steady loads are desired.

Processing Requirements

The grid system for this configuration has a total of 3.9 million points. Solutions were generated on an SGI Origin 200 with four processors and 1.8 GB of memory. Each case required about 260 MB of memory and 30 hours to converge on a single processor, except for higher angles-of-attack. These were processed further to get the solution stabilized within a certain band.

Results and Discussion

A total of six flow conditions are examined in the current study. These consist of a series of three angles-of-attack (low, mid-range and high) at two transonic Mach numbers above cruise. For each flow condition, results were obtained using the Baldwin-Barth [11] and Spalart-Allmaras [12] one-equation turbulence models, and the k-omega two-equation turbulence model [13].

Attempts to use the Menter SST model [16] were unsuccessful due to wing root grid issues. Surface pressure coefficients on the wing are presented at two stations, one inboard and one outboard. The Reynolds number matches that at which the experimental data was collected in the wind tunnel.

At low angle-of-attack, where the flow remains attached to the surface, solutions using the Baldwin-Barth model show surface pressures in very good agreement with wind tunnel data (Figure 5), with shock location and strength well predicted. Spalart-Allmaras results are similar. The k-omega model predicts a shock location significantly aft of the one-equation models. This behavior is similar to that shown in Reference 13 for transonic flow over the RAE 2822 airfoil.

For the mid-range angle-of-attack (Figure 6), Baldwin-Barth results show shock location and strength are well predicted on the upper surface inboard station for both Mach numbers and on the lower surface for the higher Mach number case. The upper surface outboard station pressure comparison shows that the shock position is about 5 percent chord aft of that measured in the wind tunnel. Here the flow separates behind the shock. For the most part the lower surface predictions are good. Toward the trailing edge, the calculated pressure coefficient shows significant unsteadiness, varying with where the solution is stopped. This is more noticeable in the high Mach number case. This behavior is not present in the Spalart-Allmaras results, where the flow is better behaved at the trailing edge. The predictions on the upper surface of the inboard station are slightly better than Baldwin-Barth. Again, the k-omega model predicts the shock location aft of the other models.

In the high angle-of-attack case (Figure 7), where a considerable amount of separation is present, the upper surface rooftop and shock location predicted by both one-equation models are fairly good. However, pressures aft of the shock at the inboard station do not match the trends of the wind tunnel data. A lower pressure at the upper surface trailing edge leads to an acceleration of the flow on the lower surface approaching the trailing edge. Results for intermediate stations (not shown here) indicate that this pattern disappears a short distance outboard of this station. This could be a result of solution convergence difficulty at these extreme conditions. Further investigation of this issue is required. Although the k-omega model continues to predict a shock location too far aft as in the previous cases, the post-shock pressure levels match wind tunnel results. The lower surface predictions for all models remain good.

Support for the aerodynamic loads process is provided by supplying design loads for various components of the aircraft such as the fuselage, nacelle, pylon, etc. This is done by providing total component load (e.g., pylon normal force coefficient), or by providing a running load.

Here, running loads are computed from the CFD solution by dividing the body into a number of segments and integrating the pressure to obtain either a force or a moment coefficient in these segments. Data can be presented either as a cumulative total starting from a specific point, or separately for each of the segments, as in Figure 8 for the fuselage. Individual component loads can also be used to determine the fraction of the aircraft total load that is being carried by a particular component (Figure 9).

If accurate, CFD solutions are invaluable for the aerodynamic loads process because they provide distributed surface pressures which can be analyzed component-by-component. These supplement wind tunnel data from extensive pressure taps or component balances, both expensive experimental techniques.

Conclusion

A Navier-Stokes flow solver, OVERFLOW, has been successfully used for the prediction of aerodynamic loads on a business jet configuration. Three turbulence models were evaluated at above-cruise Mach numbers and low to high angles-of-attack. Overall, results show the Baldwin-Barth and Spalart-Allmaras models providing the closest match to experimental results. The k-omega turbulence model predicts the shock location and flow separation farther aft

than the one-equation models. Further investigation of isolated flow patterns at the middle and high angle-of-attack cases is needed.

References

1. P.G. Buning, et al., "OVERFLOW User's Manual, Version 1.8," NASA Langley Research Center, Hampton, VA, Feb. 1998.

2. J. Samareh-Abolhassani, "GridTool: A Surface Modeling and Grid Generation Tool," NASA CP-3291, 1995.

3. S.J. Parks, P.G. Buning, J.L. Steger, and W.M. Chan, "Collar Grids for Intersecting Geometric Components Within the Chimera Overlapped Grid Scheme," AIAA 91-1587, June 1991.

4. W.M. Chan, "Manual for Chimera Grid Tools," NASA Ames Research Center, Moffett Field, CA, Oct. 1998.

5. W.M. Chan and J.L. Steger, "Enhancements of a Three-Dimensional Hyperbolic Grid Generation Scheme," Appl. Math. and Comput., Vol. 51, pp. 181-205, 1992.

6. W.M. Chan, I.-T. Chiu, and P.G. Buning, "User's Manual for the HYPGEN Hyperbolic Grid Generator and HGUI Graphical User Interface," NASA TM 108791, Oct. 1993.

7. D.G. Pearce, et al., "Development of a Large-Scale Chimera Grid System for the Space Shuttle Launch Vehicle," AIAA 93-0533, Jan. 1993.

8. R.L. Meakin, "Moving Body Overset Grid Methods for Complete Aircraft Tiltrotor Simulations," AIAA-93-3350, July 1993.

9. N.E. Suhs and R.W. Tramel, "PEGSUS 4.0 User's Manual," AEDC-TR-91-8, Arnold Engineering Development Center, Arnold AFB, TN, Nov. 1991.

10. D.C. Jespersen, T.H. Pulliam, and P.G. Buning, "Recent Enhancements to OVERFLOW," AIAA 97-0644, Jan. 1997.

11. B.S. Baldwin and T.J. Barth, "A One-Equation Turbulence Transport Model for High Reynolds Number Wall-Bounded Flows," AIAA 91-0610, Jan. 1991.

12. P.R. Spalart and S.R. Allmaras, "A One-Equation Turbulence Model for Aerodynamic Flows," La Recherche Aerospatiale, No. 1, 1994, pp. 5-21.

13. J.E. Bardina, P.G. Huang, and T.J. Coakley, "Turbulence Model Validation, Testing, and Development," NASA TM 110446, April 1997.

14. S.E. Rogers, H.V. Cao, and T.Y. Su, "Grid Generation For Complex High-Lift Configurations," AIAA 98-3011, June 1998.

15. W.M. Chan and P.G. Buning, "Surface Grid Generation Methods for Overset Grids," Computers and Fluids, Vol. 24, No. 5, 1995, pp. 509-522.

16. F.R. Menter, "Two-Equation Eddy Viscosity Turbulence Models for Engineering Applications," AIAA J., Vol. 32, Nov. 1994, pp. 1299-1310.

Figure 1: Tail-Off Chimera Grid Model of a Business Jet

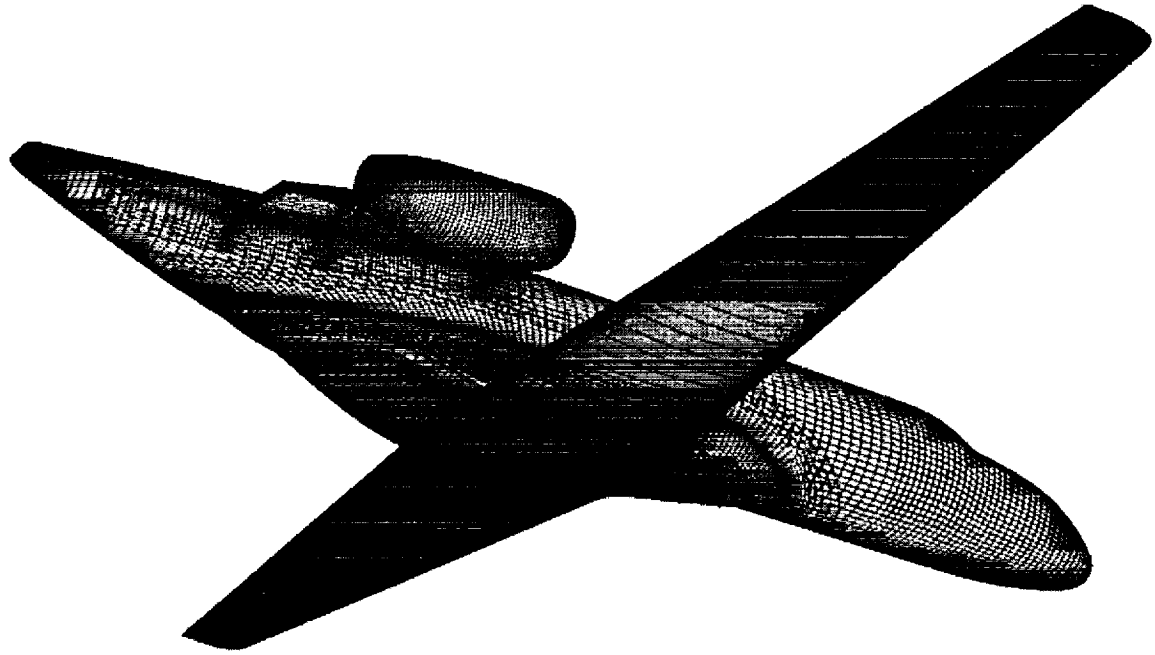

Figure 2: Wing-Body Fairing Collar Grids

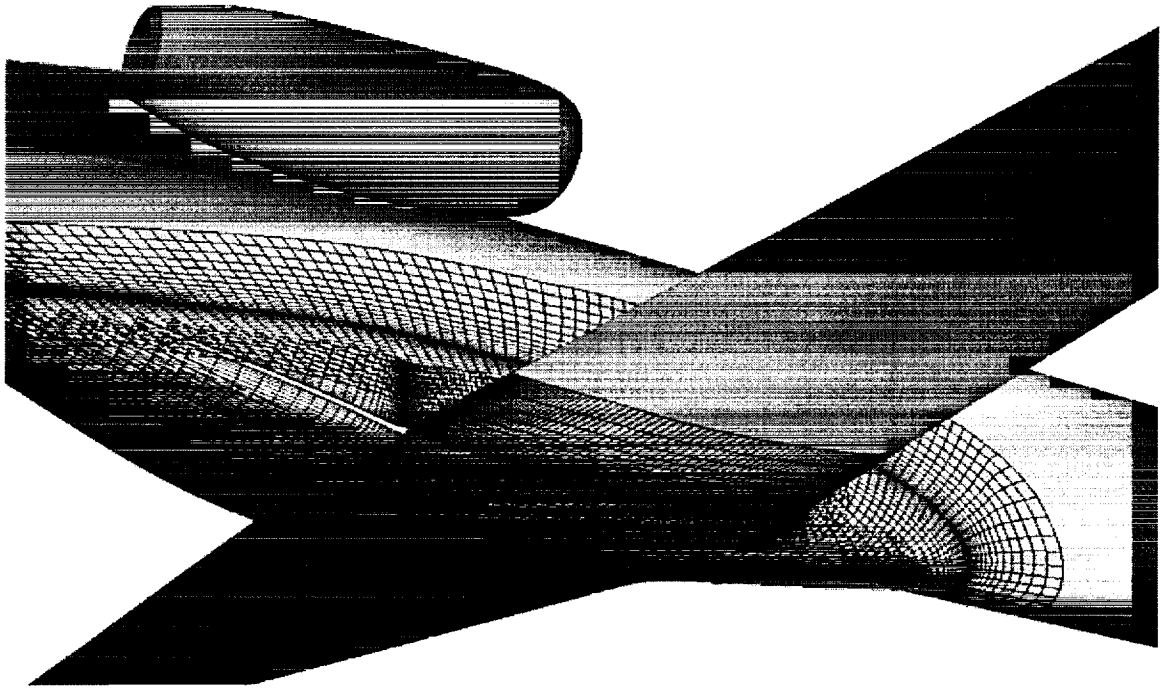

Figure 3: Pylon Shelf Cap Grid

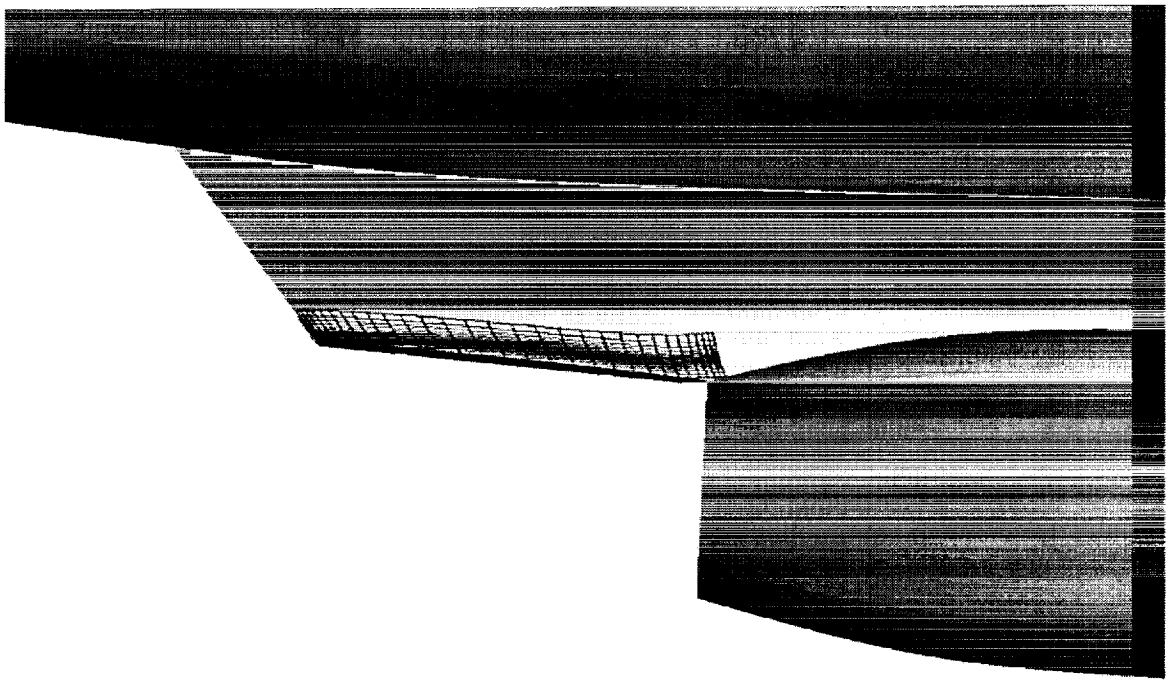

Figure 4: Wing-Body Fairing Grid Generation Process

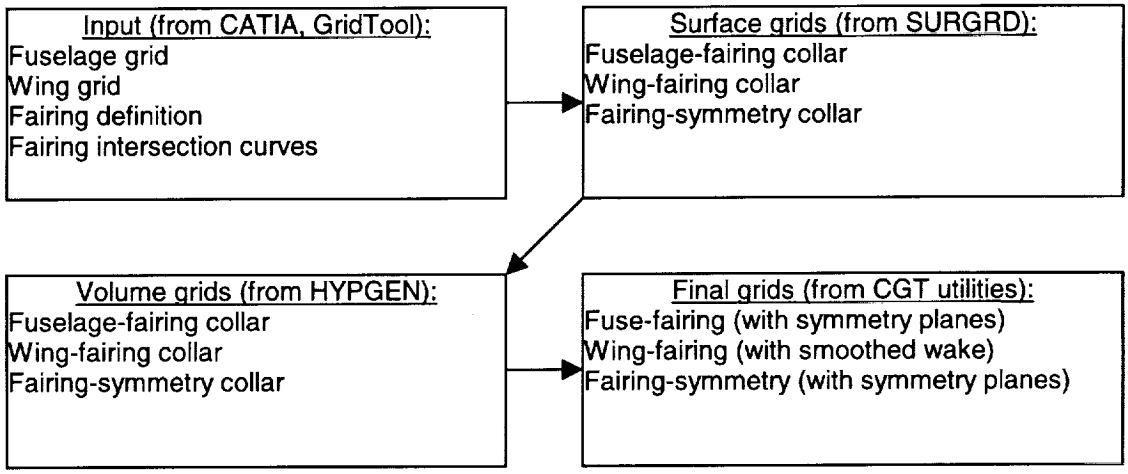

Figure 5: Predicted vs. Measured Wing Pressure Coefficient: Low Angle-of-Attack

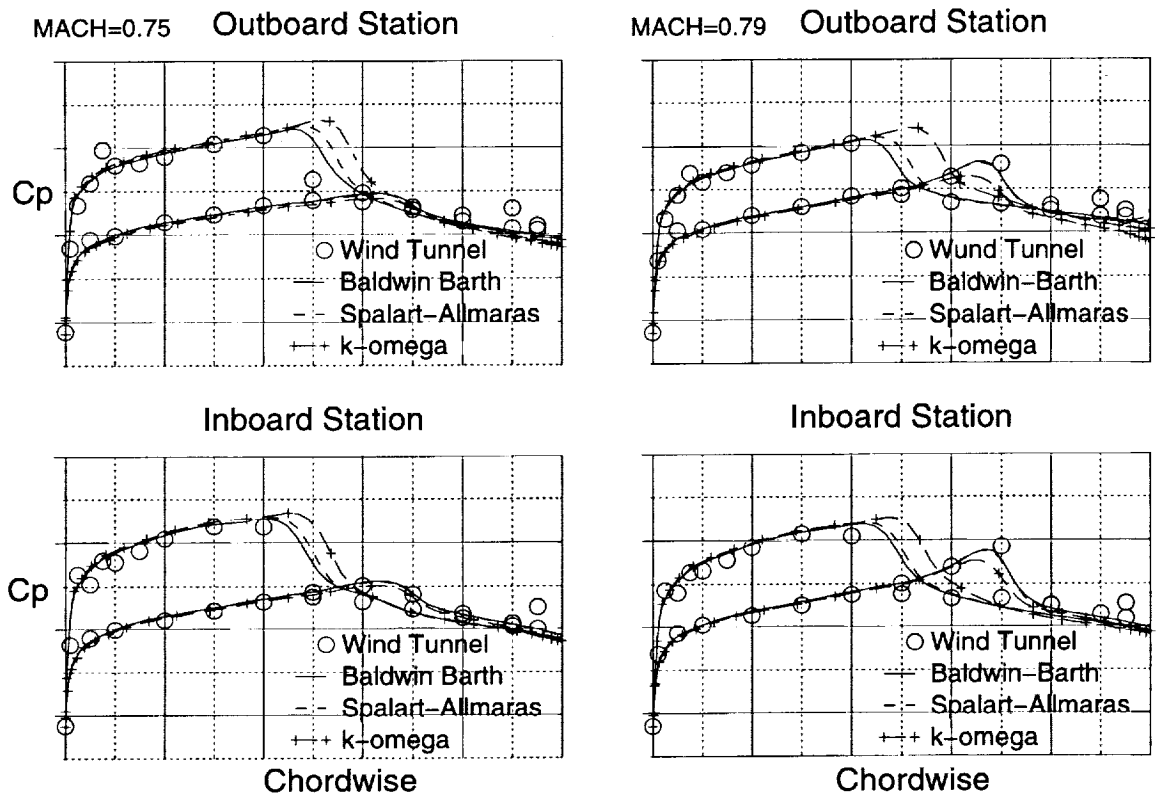

Figure 6: Predicted vs. Measured Wing Pressure Coefficient: Mid-Range Angle-of-Attack

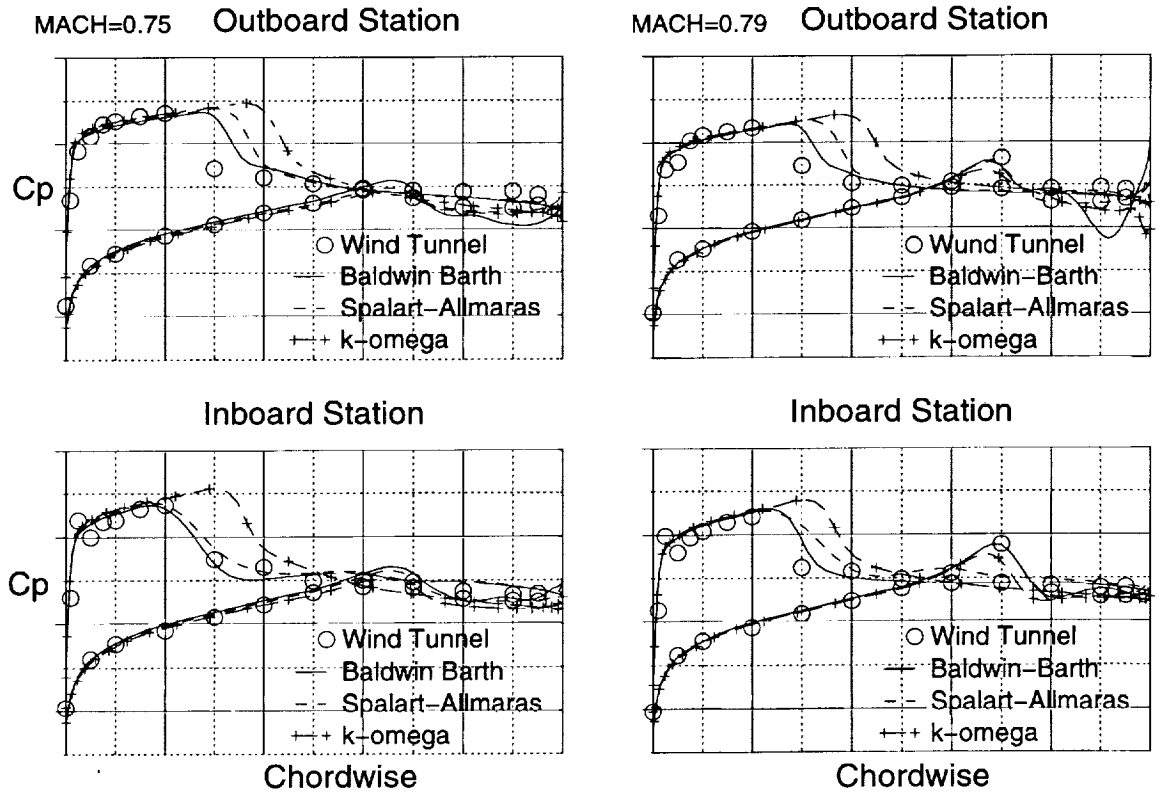

Figure 7: Predicted vs. Measured Wing Pressure Coefficient: High Angle-of-Attack

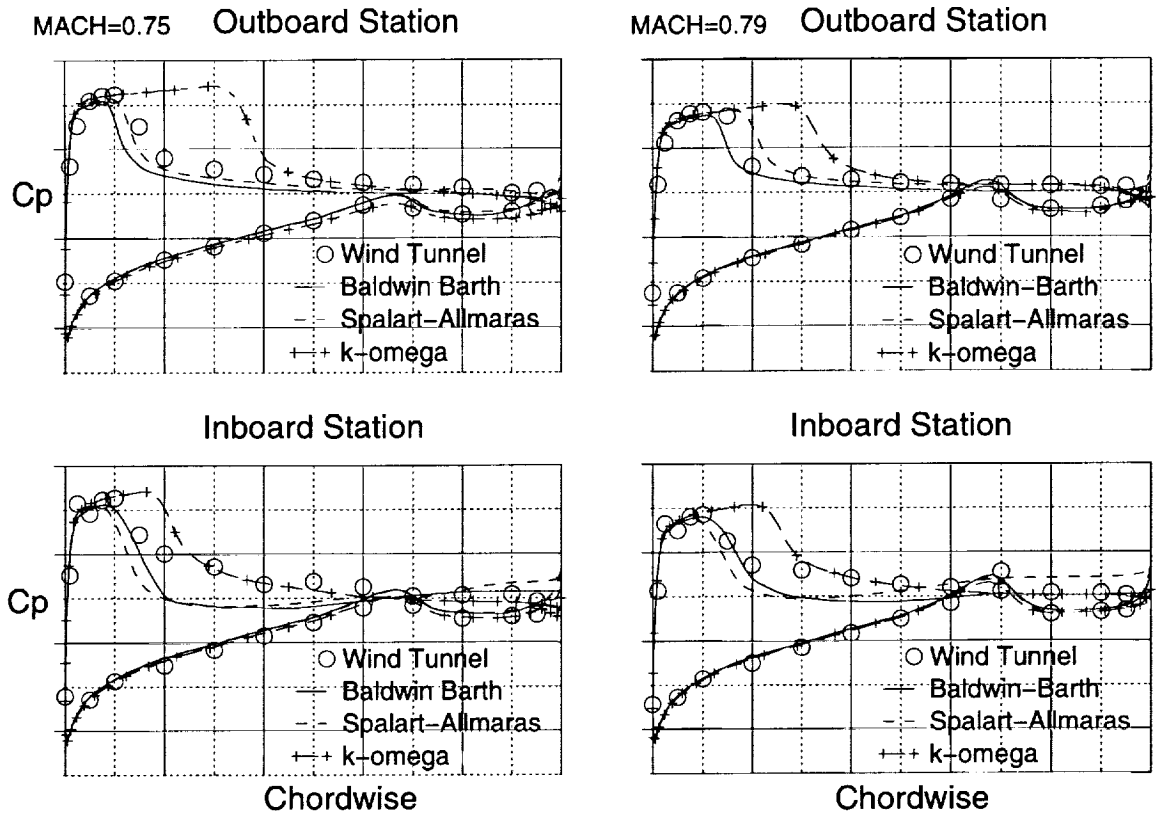

Figure 8: Fuselage Normal Force Running Load

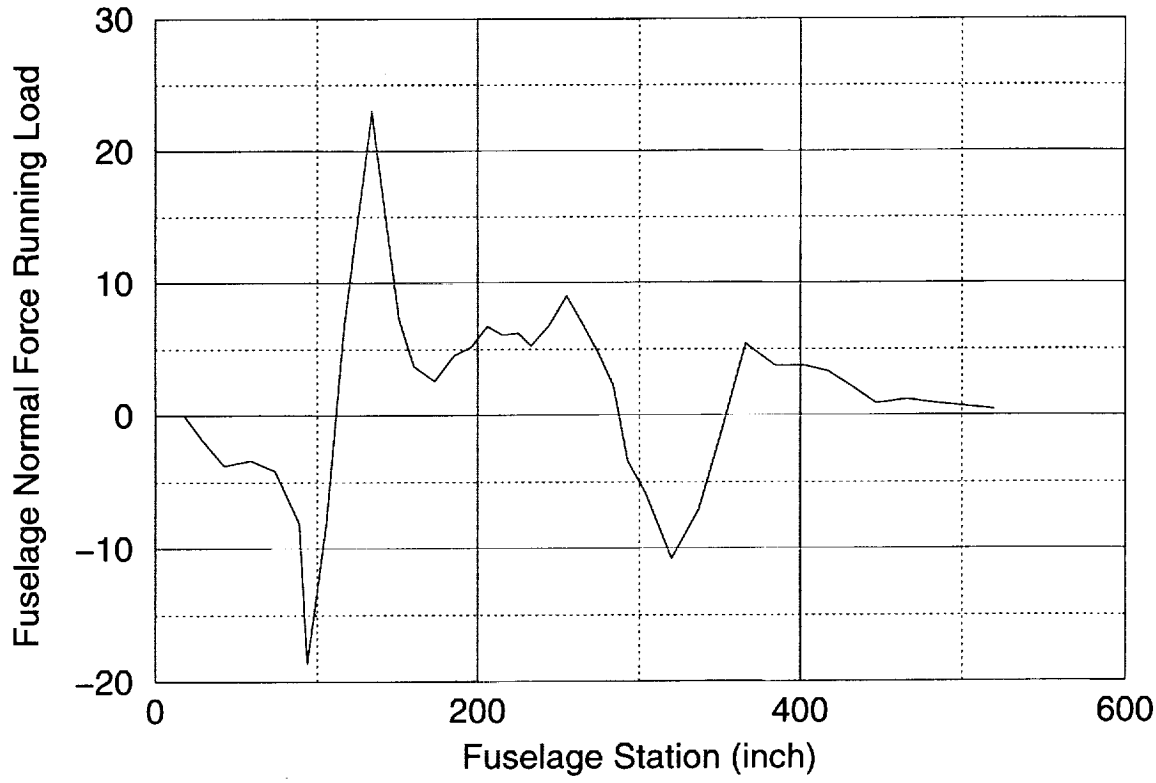

Figure 9: Aircraft Components, Percent of Total Load